SEISMIC CHARACTERIZATION OF SUBMARINE GAS HYDRATE DEPOSITS IN THE DANUBE DEEP SEA FAN (BLACK SEA) BY ACOUSTIC 2D FULL WAVEFORM INVERSION

L. Gassner and T. Bohlen

email: *laura.gassner@kit.edu*

keywords: *FWI, data application, OBS, Black Sea, gas hydrates*

ABSTRACT

To study gas hydrate deposits in the Danube Deep Sea Fan in the Black Sea off the coast of Bulgaria several geophysical experiments have been carried out including reflection and refraction seismic measurements. We aim at recovering acoustic parameters of the subsurface by applying a 2D time-domain full waveform inversion (FWI) approach to ocean bottom station (OBS) data recorded within the SUGAR-III project (SUGAR - SUbmarine GAs hydrate Resources). We utilize hydrophone data of two parallel profiles covering five stations each to study subseafloor deposits of hydrated sediments which are possibly underlain by free gas. The presence of gas hydrates and free gas is indicated by a bottom simulating reflector (BSR), which was tracked in 3D reflection seismic streamer data that was acquired in the same area as the OBS measurement.

On both profiles we invert the refracted waves at large offsets and water surface multiple reflected waves at all offsets. The high amplitude direct wave and shallow primary reflections could not be inverted because of strong artificial ringing produced by the OBS stations. As a starting model for FWI we use smooth compressional-wave velocity models obtained by travel time tomography of refracted wave first arrivals. The FWI uses frequencies of 4 Hz up to 32 Hz in a multi-stage approach. The inverted models of compressional-wave velocity have significantly higher resolution than the traveltime tomography model. At BSR-depth indications for hydrated sediments and gas are detected at the first profile. An approximately 30 m thick zone of reduced velocity in a depth agreeing with the BSR in its eastern part covering about 4.5 km is visible. Elevated velocities are found above this extended low velocity zone which indicate the presence of gas hydrates. The observed velocity drop at the BSR is approximately 200 m/s. In the central part of the second profile, high velocity anomalies are reconstructed at BSR-depth but no pronounced low-velocity zone is observed. A good overall match of the field data with the modelled seismograms for the final models could be achieved by FWI which confirms a good convergence of the inversion.

INTRODUCTION

Gas hydrates have been a topic of interest for research for a few decades with many seismic applications studying deposits by interpreting geological features to restrain gas hydrate occurrence, distribution and origin (e.g. Crutchley et al., 2011). Most applications aim at analysing the seismic signature of gas and hydrate by the so called bottom simulating reflector (BSR) which causes a strong amplitude reflection of opposite polarity compared to the seafloor reflection. It marks the base of the gas hydrate stability zone (GHSZ). With the development of continuingly bigger and faster high performance computing resources modern imaging techniques like full waveform inversion (FWI) become feasible more and more easily and allow a direct inversion of elastic parameters of the subsurface and straightforward interpretation.

First studies to characterize gas hydrate deposits by FWI originate from the 1990s and utilize a 1D approach, suggested by Singh et al. (1993). Studies by Pecher et al. (1996), Korenaga et al. (1997), and Crutchley et al. (2011) follow the 1D approach to derive v_P vs. depth relations. Recently applications of 2D FWI have been published using acoustic (Delescluse et al., 2011), visco-acoustic (Jaiswal et al., 2012) and elastic (Kim et al., 2013) approaches to study the 2D extent of gas hydrate deposits at different locations. Results suggest that hydrate occurrence can be connected to elevated P- and S-wave velocities while gas leads to a reduction of v_P only. P-wave velocities presumably characterizing gas hydrates range from 1700 m/s to 2300 m/s while values ranging from 1300 m/s to 1620 m/s for sediments containing free gas are interpreted. The vertical extent of the assumed gas layer ranges from a few meters to about 50 m (Korenaga et al., 1997). Concentration of hydrate related to the recovered parameters is estimated to be 2-6 % at 1800 m/s (LeBlanc et al., 2007) or 7-20 % at 2000-2300 m/s (Korenaga et al., 1997). Furthermore many papers relate hydrate concentration to v_P by empirical relations using weighted equation (Lee et al., 1996) or effective medium theory (Helgerud et al., 1999) giving similar results.

DATA

Regional seismic measurements have been carried out in the western Black Sea to distinguish continuous BSR horizons while geochemical measurements of watercolumn gases support the occurrence of methane hydrate enriching subseafloor sediments (https://www.migrate-cost.eu/wg1-reports, accessed: 01.12.2016). Furthermore OBS measurements have been accomplished in two areas of about 30 km^2 with additional 3D short offset seismic measurements providing high resolution information on geological horizons. In our study area seismic lines for a 2D and 3D OBS survey follow the axis of a channel levee system where hydrate deposits are likely to occur. Three profiles covering five OBS stations each are orientated along the channel axis while five profiles covering three stations each cut it perpendicular. At each station hydrophone and 3-component geophone data has been collected. The main goal of the OBS study has been structural mapping with travel time tomography of refracted wave first arrivals and converted wave P- and S-wave velocity analysis.

In the 3D reflection seismic data a BSR horizon has been tracked that covers most of the OBS station area. In figure 1 a map of the study area showing the BSR extent is presented with the geometry of the OBS measurement. For FWI hydrophone data of profiles P1 and P2 recorded at OBS 1 to 5 and 6 to 10, respectively, is utilized. Further profiles lack data quality for FWI due to high amplitude noise signals in the required frequency range. Regional seismic profiles are located between profiles P1 and P2 and P5 and P6 respectively. A 2D controlled source electromagnetic (CSEM) line has been recorded between profile P6 and P7 and modelling for converted wave velocity analysis has been done for profiles P3 and P7.

FWI APPROACH

In this work we apply an acoustic FWI approach implemented in the time-domain 2D-elastic FWI code developed by Köhn (2011). The code incorporates visco-elastic and visco-acoustic forward modelling based on a standard staggered grid finite difference (FD) scheme (Bohlen, 2002) in velocity-stress formulation. The gradients for the elastic parameters are calculated from velocity and pressure wavefields using the adjoint approach (Plessix, 2006). To enhance updates in parts of the model where illumination is poor we use a gradient preconditioning suggested by Plessix and Mulder (2004). Additionally tapers at the OBS locations are applied. Updates in the water column are suppressed and velocities are limited to the minimum and maximum values of the starting model. To reduce oscillation of model parameters a horizontal smoothing filter is applied.

The misfit of synthetic and observed pressure waveform data is defined by a L2-norm of normalised seismograms as introduced by Choi and Alkhalifah (2012). This allows to reduce uncertainties in the amplitudes of true seismograms and reduces offset dependent trade off effects which are significant especially when using an acoustic approximation. Model updates are carried out using a preconditioned conjugate gradient approach with an adaptive step length search (Kurzmann, 2012). We use frequency filtering and start from low frequencies with a highpass filter at 4 Hz, a lowpass filter at 8 Hz and increase frequency content in steps of 8 Hz up to 32 Hz during the inversion.

Due to strong ringing following the direct wave arrival time windowing is applied reducing input data to diving waves at large offsets and the first water surface multiple reflected waves (compare figure 2). Both

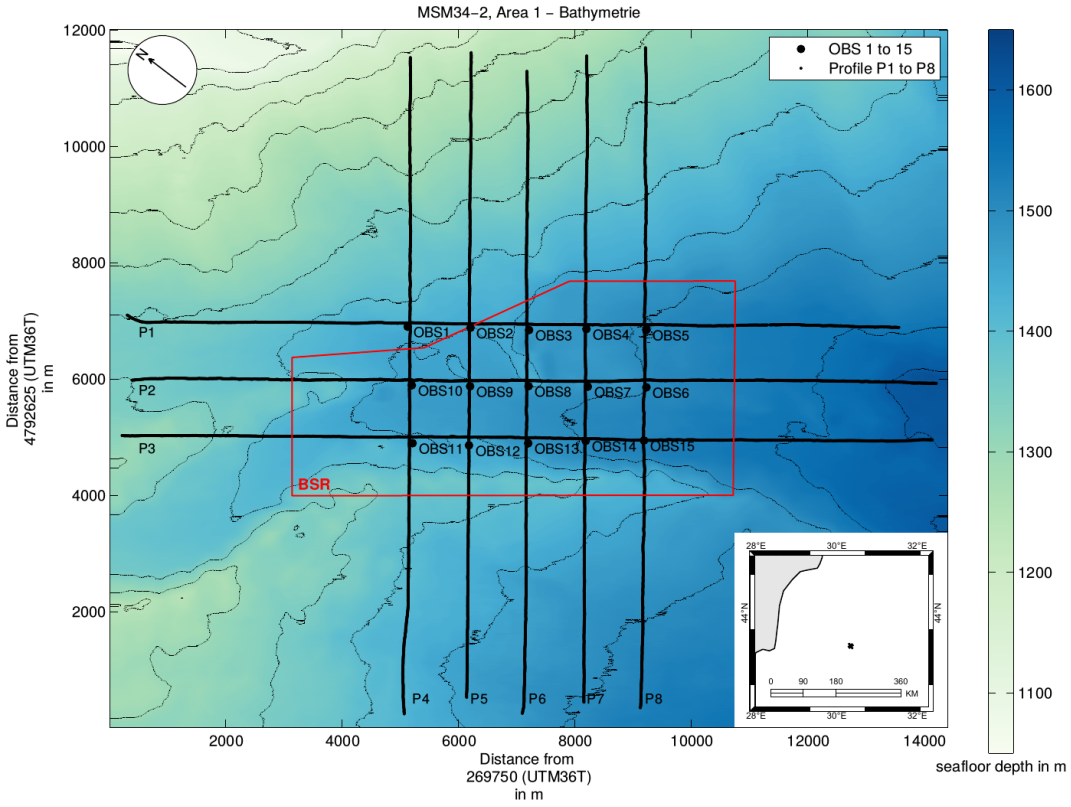

Figure 1: Bathymetric data of the study area with the geometry of the OBS measurement. Black circles mark the OBS positions and black dots the shot points (appearing as one black line per profile). The BSR outline from the 3D reflection seismic data acquired in the central part of the area is shown by the red line. For clarity coordinates were rotated by 54.5° at coordinate 269750/4792625 UTM 36T.

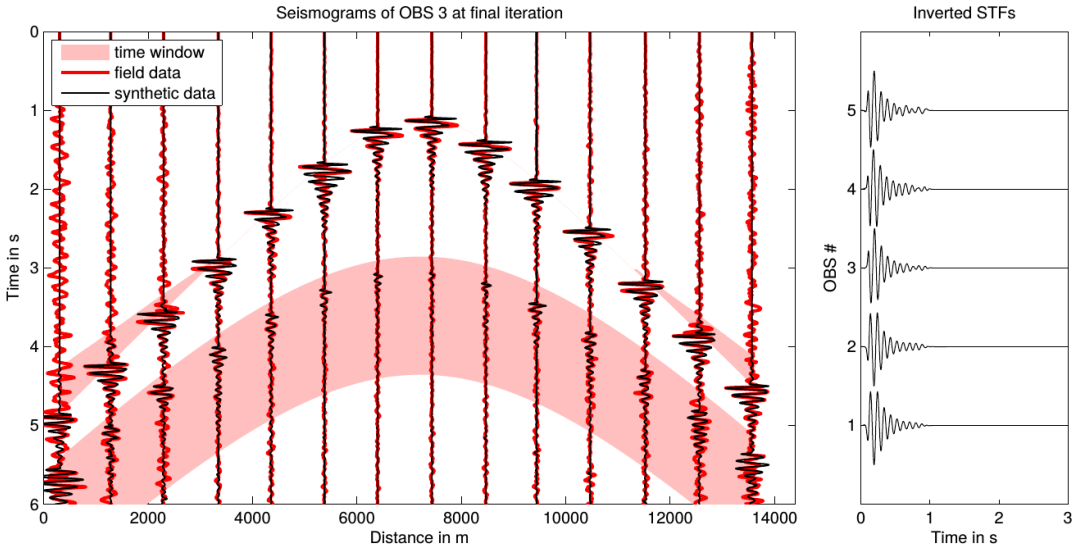

Figure 2: On the left exemplary seismograms of OBS 3 for all available offsets show the data quality and match between observed and synthetic seismograms (field data is shown in red, synthetically calculated data for the final inverted FWI model in black). The applied time window is shown in light red. On the right inverted source time functions (STFs) are shown for all five OBS stations.

wave types contribute to the outcome of the inversion while the multiple reflected waves are more sensitive to depth dependent velocity contrasts and refracted waves travel through the model in a mostly horizontal direction and therefore contain information on absolute velocity values. The high amplitude of the direct waves corrupts the inversion even if the ringing can be explained by modelled waveforms. Additionally to the v_P-inversion we apply inversion for density while we do not interpret the result. Sensitivity of seismic data is generally poor towards density especially since only normalised seismograms are considered. Density mainly incorporates contrasts at seismic interfaces while giving no resolution on absolute density values.

Source time function inversion and reciprocity

A crucial part in the FWI process is the inversion of an appropriate source time function (STF). It is carried out at the beginning of each frequency stage and consists of a waterlevel deconvolution (Forbriger, 2001). We use explosive sources describing the air gun signature and pressure receivers. This allows us to make use of the reciprocity principle for modelling and inversion. We use OBS positions as source positions and the shot positions of the measurement are used as receiver positions consequently. This approach leads to a massive reduction in calculation time as only 5 shots have to be computed instead of up to 1691 (at profile P2). A practical point is that the inverted STF describes receiver characteristics and the comparability of the inverted STF can be used as a quality control criterion.

Data preparation

In general data preparation is kept minimal for FWI to be able to match the unmodified recorded data to the synthetically calculated. A necessary data processing step is to correct for the 3D propagation characteristic of the measured OBS data. For this we use a 3D to 2D conversion suggested by Forbriger et al. (2014). It is accomplished by a convolution of each trace with $1/\sqrt{t}$ (t: traveltime) and a multiplication by $v\sqrt{2t}$ (v: velocity). As a correction velocity the sound water velocity of 1484 m/s is used. Furthermore a time shift of 0.1 s is applied which is necessary for source time function inversion. It allows to invert for a STF that contains only causal parts. A taper is applied to the inverted STF limiting it to a 1 s interval. The data is integrated in time to match the output of our inversion code and resampled to match the discretization requirements of the FD method leading to a doubling of the sampling interval to 0.5 ms. The overall recording time is 6 s for each trace while the shot spacing has been 5 s.

Starting models and geometry

OBS data of all profiles has been used to build 2D velocity models from first arrival travel time tomography of refracted wave signals. These very smooth models do not contain any information on geological units or details on possible hydrate or gas layers. They provide an overall velocity trend for the subsurface up to 3 km depth and are limited by shot and receiver coverage. We extrapolate models to the edges to acquire a model grid covering 14.4 km length. The FD discretization requirements lead to a grid point distance of 2 m meaning the model consists of a total 10.8 million grid points. At the central part of each profile five OBS stations are located with 1 km spacing. The whole profile length is covered with shots of 10 m and 8 m spacing for profiles P1 and P2 respectively. The low station coverage can therefore be compensated by the high number of shot points.

RESULTS

The acoustic FWI converges to the set abort criterion of 1 % after only 20 iterations. For the frequency stages with lowpass corner frequencies of 16 Hz and higher only the given number of minimum iterations plus one additional iteration are carried out. Most likely real data noise prevents a further misfit reduction but inversion results are satisfactory. The misfit is reduced significantly after moving to the second frequency stage because of a strong peak of the amplitude frequency spectrum of the data at 11 Hz. This frequency also limits the resolution of the inversion as wavelengths connected to this frequency are dominant. As shown in figure 2 data quality of the observed seismograms is moderate with high amplitude noise

at far offsets. The data match is good considering that only refracted and multiple wave signals have been used in the inversion. The inverted STFs for all OBS stations show high similarity.

The inverted v_P-models of profiles P1 and P2 show significantly more detail than the starting models. The smooth velocity trends from the original models has been modified towards a model where velocities are more or less constant over a whole layer being more consistent with the understanding of a subseafloor characterized by geological units. Velocity variations are visible within these layers with patches of higher and lower velocity often appearing as fluctuations of parameters with depth. These variations can be interpreted with the understanding of model updates being constructed from the correlation of wavefields. Characteristics of wave propagation will therefore also become apparent in the inverted models especially with deficits in explaining the observed wavefields by the synthetic data.

Beside mostly small amplitude variations (less than 5 % deviation from the starting model) we obtain a prominent low velocity zone at BSR depth in profile P1 coinciding with elevated velocities above it (compare figure 3(a)). Its extent is also coincident with the observed BSR horizon from 3D seismic data as it follows this horizon for about 4.5 km starting at the location of the second OBS station on this profile. The thickness of the observed low velocity layer is 30 m and the recovered contrast in v_P is about 200 m/s. In absolute values the velocity above the BSR is at around 2000 m/s while the lowest velocity is at around 1700 m/s. The inverted model deviates more than 5 % in this area compared to the starting model.

On profile P2 (compare figure 3(b)) similar observations can be made concerning the overall velocity trend which is corrected towards a model with more defined units than the starting model. In generall we observe a more pronounced velocity increase compared to the starting model than on profile P1, especially in the central model part. At BSR depth we do not observe a prominent low velocity zone as it was constructed by the inversion at profile P1. Above the BSR horizon velocities are consistently elevated in the central model part though. A zone of interest is located in the western part of the profile between the first and second OBS station (profile distances between 5 and 6 km). Here, a high velocity area above a relatively strong negative vertical velocity contrast can be observed. It is yet unclear whether free gas can occur at this depth located much higher than the bottom of the GHSZ or if hydrate accumulation can produce such a significant anomaly alone.

Sensitivity tests

To analyse the stability of the inverted v_P-model results we carried out two sensitivity tests for profile P1. The reliability of the recovered BSR signature is our main interest. First, as FWI is a local optimization method and a good starting model for the inversion is essential, we varied the starting v_P-model by 5 % and 1 % respectively. Results show that the inverted models deviate strongly from the reference solution for the 5 % starting model variation and the BSR signature can not be recovered as cycle skipping occurs. Variation of 1 % in the starting model lead to deviations in the inverted models of up to 3 % but the location and amplitude of the BSR signature can be recovered equally well (see figure 4). Variations in the density model were also investigated but as previously mentioned the sensitivity of the seismic inversion towards density is low. The influence of the density variation on the v_P-model is insignificant and density models are simply shifted by the variation amplitude of the starting model.

In another test we shifted the seafloor depth upwards by 10 m. As bathymetric data suffers from small scale variations of a few meters and depth varies between shot and OBS location lines by up to 15 m the seafloor depth corresponding to the recorded data is not reliably known. The tested seafloor shift causes 1-3 % variation in the inverted v_P-model while the changes in location and amplitude of the BSR signature is relatively small (about 1 %). All in all small changes in the starting model can lead to variations of the constructed velocity values of about 60 m/s at BSR depth.

Comparison with other methods

In the OBS study area further analysis of OBS data as well as regional seismic and 2D CSEM data has been accomplished. In the regional seismic data AVO anomalies have been observed that could not yet be linked to possible hydrate or gas occurrence. The inverted 2D CSEM resistivity models show an extended zone of high resistivity values in a depth roughly agreeing with the seismic BSR horizon. Also shallow anomalies possibly linked to hydrate or gas occurrence are observed. Further OBS studies, e.g. the analysis

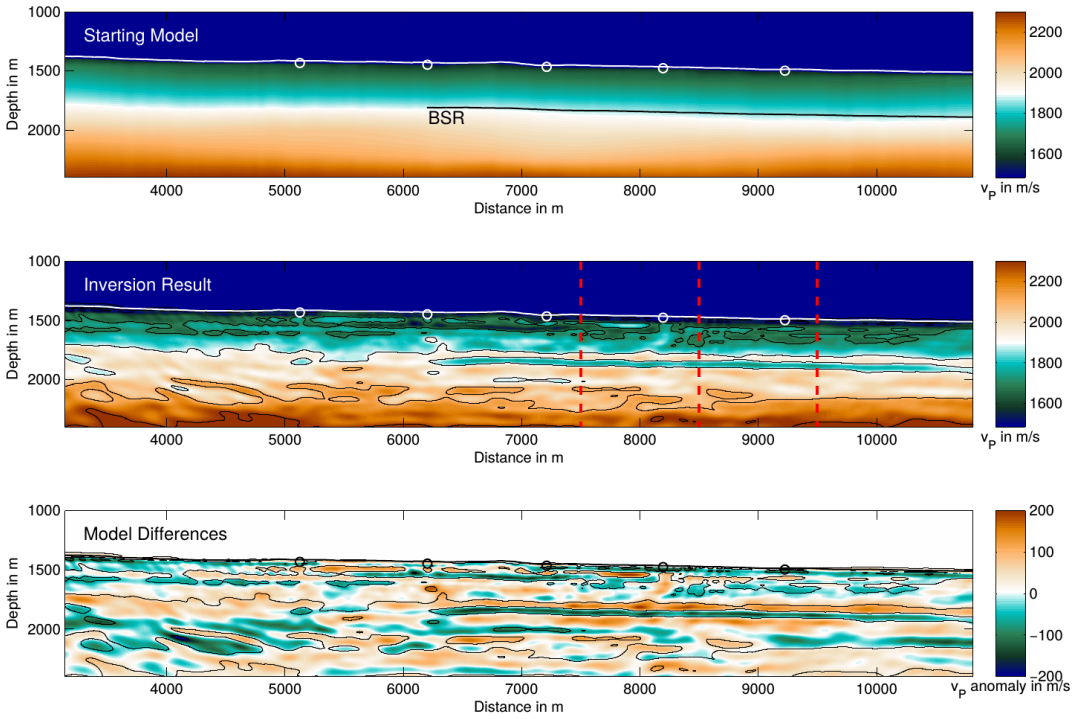

(a) Models for profile P1 show the smooth starting model with a BSR horizon observed in the eastern model part and the recovered low and elevated velocity zones at BSR depth. Red lines mark the locations of depth sections shown in figure 4.

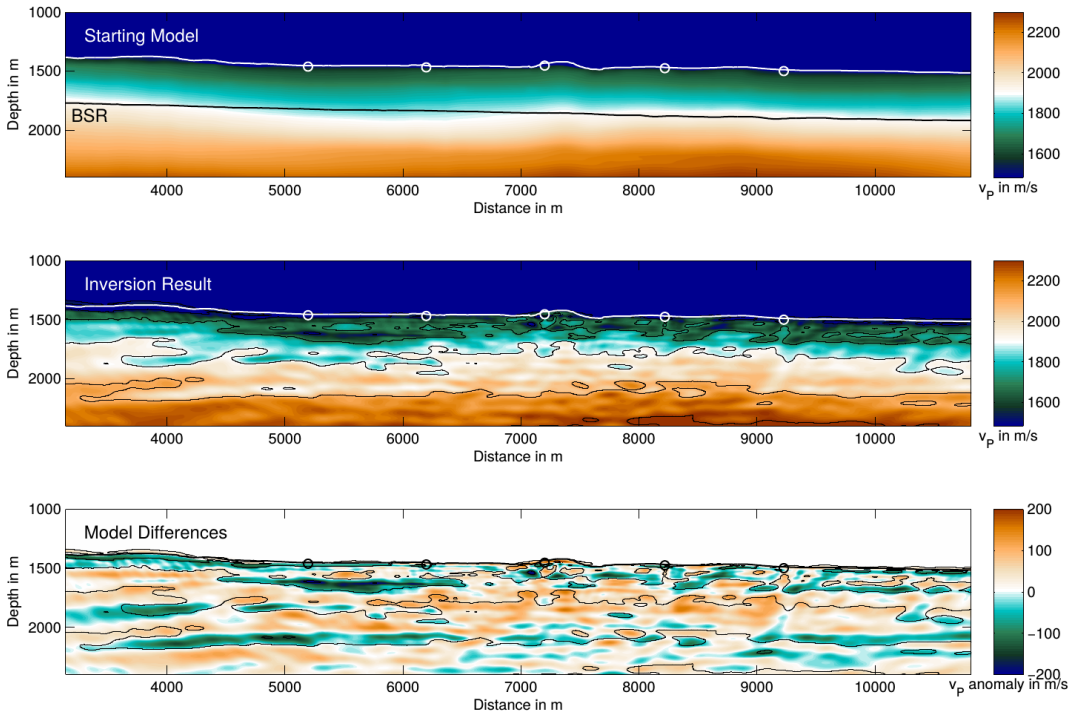

(b) Models for profile P2 with a continuos BSR horizon derived from reflection seismic data that does not appear in the inverted model. A shallow strong contrast anomaly was introduced in the western part of the profile.

Figure 3: P-wave velocity models for profile P1 and P2. Three models each show the starting model with the observed BSR horizon (upper panel), the inverted velocity model (middle panel) and the differences between the starting and final FWI model (lower panel). Black contour lines from the inverted model are projected to the model differences.

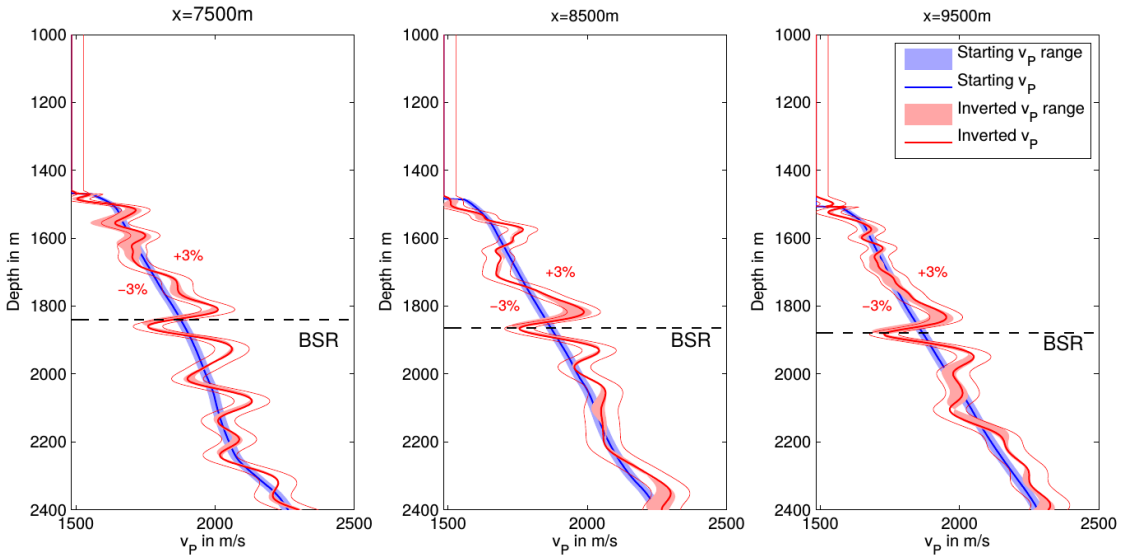

Figure 4: Depth sections for profile P1 at x=7500 m, x=8500 m and x=9500 m. A sensitivity test with 1 % v_P starting model variation (blue colors) results in up to 3 % variations in the inverted v_P-model (red colors). The location and amplitude of the BSR is constructed equally well.

of converted P-to-S-waves, give more defined models of seismic velocities interpreting a velocity reduction over the whole observed BSR horizon and anomalies at shallow depths in the central channel area. Due to the lack in overlap of the mentioned methods it is difficult yet to consistently interpret results. All results hint at hydrate and gas occurrence at BSR depth as in the FWI result of profile P1 and give the possibility to interpret shallow anomalies as observed on profile P2.

CONCLUSIONS

Results show that the 2D acoustic FWI approach is capable of constructing v_P-models that allow interpretation of the subsurface concerning the occurrence of hydrated sediments and gas layers. Even with low data quality, limited OBS coverage and reduced input data it is possible to discriminate an extensive low velocity zone which can be taken as a strong indication for gas occurrence. The high velocity zone above the BSR is then interpreted as a hydrated sediment layer. This behaviour is clearly visible on profile P1 with v_P-values agreeing well with the before mentioned literature results. Also a shallow small scale high amplitude anomaly has been observed that cannot directly be interpreted due to stronger parameter variations in the shallow subseafloor region and less complimentary information from other methods. FWI results could discriminate between a clear BSR behaviour in one of the profiles and shows no signs for a extensive gas layer at another profile though a seismic BSR signature has been observed for both areas.

In a next step we aim at applying an elastic FWI approach to allow for the inversion of a shear wave velocity model. It can provide complimentary information on subseafloor parameters and complete the characterization of possible gas hydrate deposits. Furthermore we want to study the influence of seismic attenuation on the inversion result. Many authors observed strong attenuation in sediments with increasing hydrate content implying a significant influence of attenuation on the recovered velocity models.

ACKNOWLEDGMENTS

We thank Anke Dannowski (GEOMAR) for providing the OBS travel time tomography models used as starting models for FWI. This work is carried out in the framework of the SUGAR-III project and is funded by BMWi (grant number 03SX381C).

The authors gratefully acknowledge the computing time granted on the supercomputer JURECA at Juelich Supercomputing Centre (JSC). This work was kindly supported by the sponsors of the *Wave Inver-*

sion Technology (WIT) Consortium, Karlsruhe, Germany.

REFERENCES

Bohlen, T. (2002). Parallel 3-d viscoelastic finite difference seismic modelling. *Computers & Geosciences*, 28(8):887–899.

Choi, Y. and Alkhalifah, T. (2012). Application of multi-source waveform inversion to marine streamer data using the global correlation norm. *Geophysical Prospecting*, 60(4):748–758.

Crutchley, G., Gorman, A., Pecher, I., Toulmin, S., and Henrys, S. (2011). Geological controls on focused fluid flow through the gas hydrate stability zone on the southern hikurangi margin of new zealand, evidenced from multi-channel seismic data. *Marine and Petroleum Geology*, 28(10):1915–1931.

Delescluse, M., Nedimović, M. R., and Louden, K. E. (2011). 2d waveform tomography applied to long-streamer mcs data from the scotian slope. *Geophysics*, 76(4):B151–B163.

Forbriger, T. (2001). Inversion flachseismischer Wellenfeldspektren.

Forbriger, T., Groos, L., and Schäfer, M. (2014). Line-source simulation for shallow-seismic data. part 1: Theoretical background. *Geophysical Journal International*, 198(3):1387–1404.

Helgerud, M., Dvorkin, J., Nur, A., Sakai, A., and Collett, T. (1999). Elastic-wave velocity in marine sediments with gas hydrates: Effective medium modeling. *Geophysical Research Letters*, 26(13):2021–2024.

Jaiswal, P., Dewangan, P., Ramprasad, T., and Zelt, C. (2012). Seismic characterization of hydrates in faulted, fine-grained sediments of krishna-godavari basin: Full waveform inversion. *Journal of Geophysical Research: Solid Earth (1978–2012)*, 117(B10).

Kim, H.-J., Jou, H.-T., Kang, S.-G., Lee, G. H., Yi, B. Y., Yoo, D.-G., Ryu, B.-J., and Shin, C. (2013). Seismic characterization and imaging of a gas hydrate deposit in the western part of the ulleung basin, the east sea (japan sea). *Marine and Petroleum Geology*, 47:214–221.

Köhn, D. (2011). Time domain 2d elastic full waveform tomography. *Ph. D. dissertation*.

Korenaga, J., Holbrook, W., Singh, S., and Minshull, T. (1997). Natural gas hydrates on the southeast us margin: Constraints from full waveform and travel time inversions of wide-angle seismic data. *Journal of Geophysical Research: Solid Earth (1978–2012)*, 102(B7):15345–15365.

Kurzmann, A. (2012). *Applications of 2D and 3D full waveform tomography in acoustic and viscoacoustic complex media*. PhD thesis, Karlsruhe, Karlsruher Institut für Technologie (KIT), Diss., 2012.

LeBlanc, C., Louden, K., and Mosher, D. (2007). Gas hydrates off eastern canada: Velocity models from wide-angle seismic profiles on the scotian slope. *Marine and Petroleum Geology*, 24(5):321–335.

Lee, M., Hutchinson, D., Collett, T., and Dillon, W. P. (1996). Seismic velocities for hydrate-bearing sediments using weighted equation. *Journal of Geophysical Research: Solid Earth*, 101(B9):20347–20358.

Pecher, I. A., Minshull, T. A., Singh, S. C., and von Huene, R. (1996). Velocity structure of a bottom simulating reflector offshore peru: Results from full waveform inversion. *Earth and Planetary Science Letters*, 139(3):459–469.

Plessix, R.-E. (2006). A review of the adjoint-state method for computing the gradient of a functional with geophysical applications. *Geophysical Journal International*, 167(2):495–503.

Plessix, R.-E. and Mulder, W. (2004). Frequency-domain finite-difference amplitude-preserving migration. *Geophysical Journal International*, 157(3):975–987.

Singh, S. C., Minshull, T. A., and Spence, G. D. (1993). Velocity structure of a gas hydrate reflector. *SCIENCE-NEW YORK THEN WASHINGTON-*, 260:204–204.